Organic & Biomolecular Chemistry

Cite this: *Org. Biomol. Chem.*, 2012, **10**, 3617

www.rsc.org/obc

PAPER

Optical and electrochemical properties of heteroditopic ion receptors derived from crown ether-based calix[4]arene with amido-anthraquinone pendants†

Benjamat Chailap and Thawatchai Tuntulani*

Received 9th January 2012, Accepted 6th March 2012
DOI: 10.1039/c2ob00048b

Two heteroditopic receptors based on a calix[4]arene crown ether containing amidoanthraquinone pendants in cone and 1,3-alternate conformations (**1** and **2**, respectively) were synthesized. Photophysical properties of **1** and **2** were studied by UV-vis and fluorescence spectrophotometry in dried CH_3CN. Both **1** and **2** showed the highest sensitivity towards F^- through the appearance of a new charge transfer band at 500 nm and the enhancement of the emission spectra at λ_{em} = 542 nm and 528 nm respectively. Interestingly, in the presence of K^+, the fluorescence intensity of **1** at 542 nm increased around 2 fold compared to that in the absence of K^+ upon addition of F^-, while this phenomenon was not observed in the case of receptor **2**. Cyclic voltammograms of receptors **1** and **2** showed two consecutive one-electron reversible waves in 40% v/v CH_3CN in CH_2Cl_2, corresponding to two single-electron reductions to give mono- and dianions species at $E_{1/2}$I = −1.21 V and $E_{1/2}$II = −1.66 V as well as $E_{1/2}$I = −1.25 V and $E_{1/2}$II = −1.71 V, respectively. $H_2PO_4^-$ gave remarkable potential shifts (*ca*. 200 mV) of the second reduction waves ($E_{1/2}$II) of both free **1** and **2**. In the presence of K^+, only receptor **1** gave remarkable potential shifts in its redox wave II upon adding F^- and AcO^-. Therefore, receptors **1** and **2** exhibited dual sensing modes by fluorescence spectrophotometry and cyclic voltammetry. The topology of ligands also played an important role in cooperative binding properties of heteroditopic receptor **1** possessing a closer distance between a cation and an anion binding. On the other hand, the two ion binding sites of receptor **2** were separated by a longer distance and did not support the cooperative binding. This resulted in the abstraction of K^+ from receptor **2** upon addition of anions.

Introduction

In the past decade, anthraquinone, a well-known important dye, has been applied as a sensory unit in chemical sensors.[1–20] A number of anthraquinone derivatives showed optical signals upon interacting with metal ions such as Cu^{2+},[2–10] Ni^{2+},[9] Al^{3+},[11] In^{3+},[12] and Hg^{2+},[13] through their coordination or deprotonation at the binding sites. However, most anion sensors based on anthraquinone exhibited high selectivities towards fluoride and acetate ions.[14–20] Most of the reported anthraquinone derivatives for detecting fluoride ions employed various signal transductions such as charge transfer bands in UV/vis spectra, color changes and emission spectra from excited-state intramolecular proton transfer (ESIPT).[14–20] The mechanisms of the signal transductions were mainly due to the deprotonation[14–16] or hydrogen bonding interactions[17–20] between fluoride ion and the functional groups such as urea, thiourea as well as imidazolium salts. Besides signals from optical spectroscopy, anthraquinone derivatives displayed electrochemical signals as well. The quinone group gave two successive single electron reduction steps, Q^{1-} and Q^{2-}, leading to two reversible redox waves in the cyclic voltammogram.[21–24] Addition of fluoride ions into the solution of anthraquinone attached with two amido benzene groups led to fluoride ions and quinone oxygen competing to form hydrogen bonds with amide groups, resulting in remarkable changes in its electrochemical signals.[25] Recently, dual redox and fluorescent sensors have become an interesting subject due to their multi-channel for sensing ions. They can sense ions through not only the fluorescence changing but also the shift of redox potentials, anodically or cathodically.[26–30] Hardouin-Lerouge *et al*. have recently reported tetrathiafulvalene–phenanthroline derivative exhibiting as a dual redox and colorimetric sensor for various cations.[30] From this point of view, anthraquinone is an interesting dual mode unit for sensing ions because of its diverse optical and electrochemical properties. In addition, sensors bearing anthraquinone moieties that display the dual ion-sensing mode are still rarely reported.

Department of Chemistry, Faculty of Science, Chulalongkorn University, Phyathai Road, Bangkok, 10330, Thailand. E-mail: tthawatc@chula.ac.th; Fax: +66 2-2541309; Tel: +66 2-2187643

†Electronic supplementary information (ESI) available: ^{1}H NMR and ^{13}C NMR spectra of compounds **1a**, **2a**, **1** and **2**, Job's plots, UV-vis and fluorescence spectra and cyclic voltammograms. See DOI: 10.1039/c2ob00048b

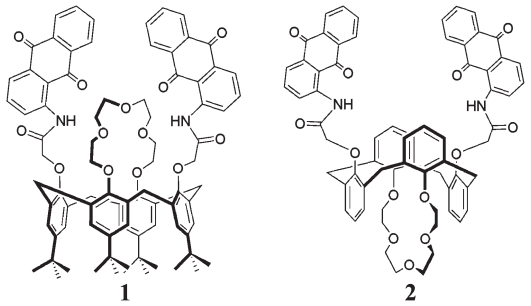

Fig. 1 Structures of receptors **1** and **2**.

Compared to simple anion receptors, heteroditopic or ion-pair receptors generally display significantly enhanced affinities towards anions stemming from cooperative or allosteric effects which attributes to the electrostatic interactions from different charged ions bound to the receptors.[31–41] Calix[4]arene is one of the most suitable synthetic macrocycles for the design of ion-pair receptors since various functional groups can be modified to its wide and narrow rim. Moreover, calix[4]arene derivatives exist in many conformations. Therefore, the space between two functional groups can be varied.[31,32] In this study, two heteroditopic ion receptors based on amidoanthraquinone-crown ether calix[4]arene in cone conformation and 1,3-alternate conformation, **1** and **2**, respectively have been synthesized (Fig. 1). We expect that the combination of amidoanthraquinone and calix-crown ether in different conformations would result in an optimized structure for the ion-pair system to enhance the anion affinity, recognition and sensing. Furthermore, we also expect that the quinone moiety could exhibit dual sensing modes, both optical and electrochemical responses, which may be useful for monitoring specific ions.

Results and discussion

Synthesis of receptors 1 and 2

The synthetic procedures for receptors **1** and **2** are shown in Scheme 1. Substitution reaction of *p-tert*-butylcalix[4]arene with tetraethyleneglycol ditosylate (prepared from tetraethylene glycol) using K_2CO_3 as base in CH_3CN gave **1a** in 40% yield. Compound **1a** was then reacted with bromoacetyl amidoanthraquinone in the presence of K_2CO_3 in acetonitrile at reflux to give **1** in 9% yield. Using a similar method, substitution reaction of calix[4]arene with bromoacetyl amidoanthraquinone using K_2CO_3 as base in CH_3CN at reflux gave **2a** in 32% yield. Compound **2a** was then reacted with tetraethyleneglycol ditosylate in the presence of Cs_2CO_3 in acetonitrile at reflux to give **2** in 7% yield. Both compounds **1** and **2** were characterized by NMR spectroscopy (Fig. S1–S8 in ESI†), mass spectrometry and elemental analysis. The ^{1}H NMR spectrum of **1** suggests that the calix[4]arene unit is in a cone conformation according to the characteristic of cone conformation, the Ar*CH*$_2$Ar signals, which appear as a pair of doublets (Ar–CH_2–Ar AB system) at 4.73 and 3.27 ppm (J = 12.8 Hz). The ^{13}C NMR spectrum of **1** shows a signal of *syn* Ar_2CH_2 around 31 ppm.[42] For receptor **2**, the conformation of calix[4]arene is assigned as 1,3-alternate. Even

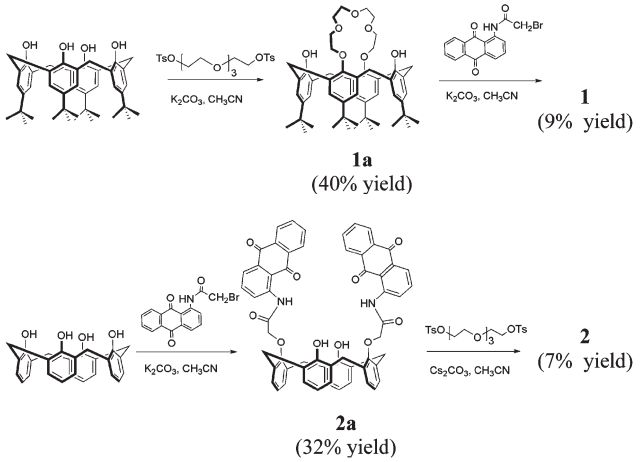

Scheme 1 Synthetic procedure of receptors **1** and **2**.

though a pair of doublet Ar*CH*$_2$Ar signals appear at 3.90 and 4.20 ppm (J = 16.4 Hz), the characteristic *anti* Ar_2CH_2 appears at around 38 ppm in the ^{13}C NMR spectrum, which supports the 1,3-alternate conformation of the calix[4]arene framework in **2**.[42] In addition, the chemical shift of the NH amide proton of receptors **1** and **2** appears in the downfield region at 12.40 and 12.23 ppm, respectively, suggesting intramolecular hydrogen bonding. This indicates that intramolecular hydrogen bonding interactions of the amide groups and the oxygen of anthraquinone could occur.[14,16] Interestingly, the amide protons of **1** shift to a more downfield region than those of **2**, implying that intramolecular hydrogen bonding interactions in **1** are stronger than those in **2**. This is probably due to the crown ether group in **1** involving in H-bonding interactions.

Complexation studies of receptors 1 and 2 by ^{1}H NMR titrations

The cation recognition of receptors **1** and **2** was investigated by using ^{1}H NMR titrations. The ability of receptors **1** and **2** to bind metal salts was observed in 5% v/v CD_3CN in $CDCl_3$ through titrations with $NaClO_4$ and KPF_6. It was found that two sets of resonances were observed for all the proton signals in the ^{1}H NMR spectra of **1** and **2** (Fig. S9 and S10 in ESI†), resulting from strong binding interactions with a slow complexation behavior. The receptor–cation complexes form completely upon addition of 1 equivalent of cations, which are consistent with a 1 : 1 binding mode. Binding constants were determined by direct integration of signals from free receptors and complexes in ^{1}H NMR spectra as described by Macober.[43] It was found that both receptors showed higher binding constants towards K^+ than those towards Na^+ as shown in Table 1. These results are consistent with the previous study that reported the polyether ring of calix[4]crown-5 was more suitable for complexing K^+.[44] According to these binding constants, co-bound K^+ complexes are chosen to study the cooperative binding of receptors **1** and **2** with anions.

The ability of receptors **1** and **2** to bind anions (added as their tetrabutylammonium salt) was tested in 5% $CD_3CN/CDCl_3$. In the absence of K^+, the amide-NH protons of receptors **1** and **2** shift slightly downfield and disappeared after addition of

Table 1 Binding constants derived from ^{1}H NMR titration

	Binding constants (M^{-1})[a]	
Receptor	Na^+	K^+
1	330	2700
2	250	2650

[a] Maximum error estimated to be less than ±10%.

1 equivalent of fluoride ion. These results indicate the formation of hydrogen-bond complex between those receptors and F^-. Furthermore, after excess fluoride ions (4 equiv.) are added, no 1 : 2 : 1 triplet signal around 16 ppm, which is ascribed to the FHF^- species, is found.[14] This result supports the formation of hydrogen bonds occurring, rather than the deprotonation.[18,19] No changes in ^{1}H NMR spectra are detectable for other anions. Thus, it implies that receptors **1** and **2** prefer binding with F^-.

The anion binding studies of receptors **1** and **2** in the presence of K^+ were carried out in 5% v/v CD_3CN in $CDCl_3$. The results show that most anions cause the abstraction of K^+ from the receptors. Only AcO^- gave slight shifts of NH signals. Therefore, the cooperative binding is further studied by photophysical methods and electrochemistry.

Photophysical properties and ion recognition abilities of compounds 1 and 2

Anion sensing abilities of **1** and **2** can be observed through their photophysical properties in the absence and presence of cations in dried CH_3CN using UV-vis and fluorescence spectrophotometry. The UV-vis spectrum of **1** shows an absorption band at 400 nm which is ascribed to the π–π* transition of the chromophore.[14] Anion sensing abilities of the sensors are examined by adding the excess of tetrabutylammonium salts (50 equiv.) of anions (F^-, Cl^-, Br^-, I^-, BzO^-, AcO^-, $H_2PO_4^-$) to a dried CH_3CN solution of sensors. The addition of fluoride ion produces a new absorption band at 500 nm (Fig. 2a) and results in color change from pale yellow to pale orange after adding fluoride ion up to 50 equiv., while other anions show only insignificant decrease in an absorption band at 400 nm and do not cause any changes in color. The new absorption band corresponds to the charge transfer (CT) band between the electron-rich amide-bound F^- and the electron-deficient anthraquinone moieties.[14,15,17,19,20]

The UV-vis spectra of **1** and **2** with potassium ions display a slight hypsochromic shift of the absorption maximum (from 400 nm to 392 nm). Anion sensing abilities of receptors **1** and **2** in the presence of K^+ are carried out by adding 1.2 equiv. of K^+ (added as potassium hexafluorophosphate) to the solution of receptors. The intensity of the charge transfer band at 500 nm is distinctively increasing upon addition of fluoride ion into the solution of [**1**·K^+] as shown in Fig. 2.

Interestingly, addition of only 10 equivalents of fluoride ion to the solution of [**1**·K^+] solution causes a color change from pale yellow to orange as shown in Fig. 3a, while the addition of the same equivalents of fluoride ion to the free receptor **1** solution does not cause any changes in color. The result may stem from

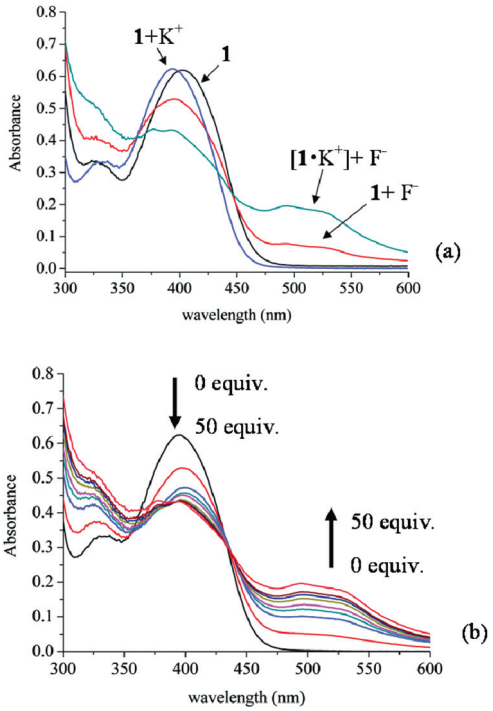

Fig. 2 (a) UV-vis spectra of **1** (50 μM) and TBAF·$3H_2O$ (50 equiv.) in the absence (red spectrum) and presence (green spectrum) of KPF_6 (1.2 equiv.) in CH_3CN. (b) UV-vis titration spectra of **1** (50 μM) + KPF_6 (1.2 equiv.) upon addition of TBAF·$3H_2O$ in CH_3CN.

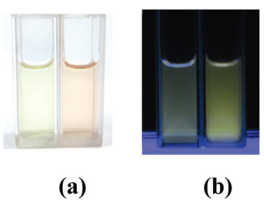

Fig. 3 (a) Color and (b) fluorescence emission of chemosensor [**1**·K^+] (50 μM+K^+ 1.2 equiv.) before and after the addition of TBAF·$3H_2O$ (10 equiv.) in CH_3CN.

K^+ residing in the crown ether cavity causing electrostatic interactions with F^- as well as cooperative hydrogen bonding interactions between F^- and the amide groups. Other anions cause no distinct difference to π–π* transition or charge transfer bands in [**1**·K^+] spectra. UV-visible studies of receptor **2** show similar results to the receptor **1**. However, K^+ does not lead to a remarkable increase in the band at 500 nm of [**2**·K^+] as much as the band found in the case of [**1**·K^+] (Fig. S11 in ESI†).

Previous studies of anthraquinone derivatives showed that excited-state intramolecular proton transfer (ESIPT) existed as dual fluorescence emissions: short-wavelength emission (SWE) band around 520 nm for the normal structure and long-wavelength emission (LWE) around 560 nm for the tautomer structure.[14,20] Jung *et al.* reported a fluorescent chemosensor consisting of two 1-amidoanthraquinone units linked to calix[4] arene.[20] It was found that, fluoride ion caused the inhibition of ESIPT which could be observed through the remarkable increase in a normal band of emission spectra, while the band of tautomer

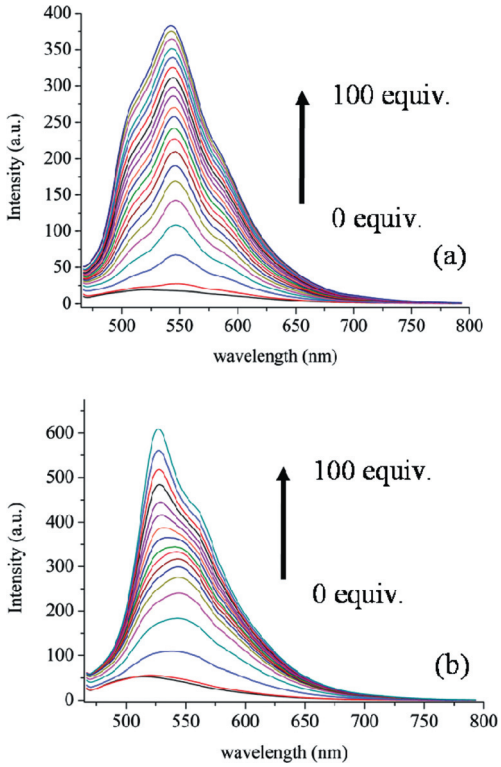

Fig. 4 Fluorescence emission spectra of (a) **1** (50 μM) and (b) **2** (50 μM) upon gradual addition of TBAF·3H$_2$O in CH$_3$CN from 0 to 100 equiv. λ_{ex} at 450 nm.

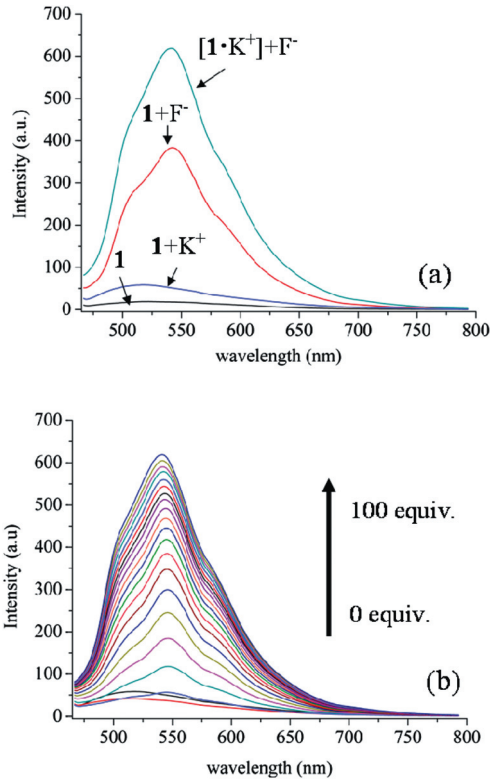

Fig. 5 (a) Fluorescence emission spectra of **1** (50 μM) and TBAF·3H$_2$O (100 equiv.) in the absence (red spectrum) and presence (green spectrum) of KPF$_6$ (1.2 equiv.) in CH$_3$CN. (b) Fluorescence titration spectra of **1**(50 μM) + KPF$_6$ (1.2 equiv.) upon addition of TBAF·3H$_2$O (0–100 equiv.) in CH$_3$CN. λ_{ex} at 450 nm.

structure was slightly changed upon addition of fluoride. The reason was due to the formation of intramolecular H-bonding between fluoride ions and amide groups (or deprotonation) which promoted the delocalization of π-electrons through the 1-amidoanthraquinone, causing changes in the π–π* transition.

Since free **1** and **2** do not exhibit LWE by changing solvent polarity or donicity, no ESIPT proceeds in free receptors (Fig. S11 in ESI†). Emission spectra of receptors **1** and **2** in the presence of fluoride ion are measured in CH$_3$CN and shown in Fig. 4. The free **1** exhibits a weak emission maximum at 520 nm, while the emission maximum shifts to 542 nm after the addition of fluoride ion. Similarly, receptor **2** also shows the highest sensitivity with fluoride ions. Excess of fluoride ion gives emission spectra at 528 nm with a shoulder at 560 nm. The high selectivity of **1** and **2** with F^- ion is probably due to the formation of intramolecular H-bonds between NH and F^- which promotes the delocalization of π-electrons through the 1-aminoanthraquinone.[20]

In the presence of 1.2 equivalents of K^+, [**1**·K^+] still shows high selectivity with F^-. However, compared to the spectrum of **1**, the [**1**·K^+] spectrum shows around two-fold higher intensity in the presence of equal equivalents of added fluoride ion as shown in Fig. 5a. This phenomenon is similar to the previous study reported by Senthilvelan *et al.* A calix[4] arene derivative showed further enhancement of its fluorescence intensity upon complexation with acetate or fluoride ions in the presence of Cu(I).[41] In contrast, receptor **2** shows lower sensitivity towards F^- in the presence of K^+ (Fig. S12 in ESI†). This observation is also supported by the association constants which are calculated by SPECFIT32 software and listed in Table 2. Data fitting and refining, Job's plots as well as fitting graphs (Fig. S13–S17 in ESI†) suggest that receptor **1** and [**1**·K^+] bind F^- in two stepwise fashions, a 1 : 1 following by a 1 : 2 fashion, while receptor **2** forms a 1 : 1 complex with F^-. It was found that the association constant value for [**1**·K^+] and F^- is higher than that of free **1** and F^- confirming that K^+ plays a key role in the sensitivity of **1** with F^-. As a consequence, the results imply that K^+ residing in the crown ether of **1** supports the formation of intermolecular H-bonds between the amide protons and F^- ions resulting in promoting the delocalization π-electrons through the anthraquinone moiety and causing changes in π–π* transition with a fluorescence color change from pale yellow to bright yellow as shown in Fig. 3b. Unfortunately, the association constant

Table 2 Association constants for receptors **1** and **2** with F^- in the presence and in the absence of cation

	Binding constants	
Receptor + anion	Log K_1	Log K_2
1 + F^-	2.94 ± 0.04	4.50 ± 0.03
[**1**·K^+] + F^-	3.39 ± 0.12	6.25 ± 0.05
2 + F^-	3.77 ± 0.14	—
[**2**·K^+] + F^-	[a]	[a]

[a] Cannot be calculated due to the abstraction of K^+ by F^-.

Table 3 Changes in reduction potentials (mV) of receptors **1** and **2** after addition of various anions (10 equiv.)

	Receptors			
	1		**2**	
Anions	$\Delta E_{1/2}$ (I)	$\Delta E_{1/2}$ (II)	$\Delta E_{1/2}$ (I)	$\Delta E_{1/2}$ (II)
F^-	15	25	50	35
Cl^-	20	15	25	30
Br^-	0	20	30	5
I^-	15	10	40	30
AcO^-	15	10	40	30
BzO^-	25	5	40	45
$H_2PO_4^-$	5	195	20	215

$\Delta E_{1/2} = E_{1/2\ \text{anion cpx}} - E_{1/2\ \text{free receptor}}$.

between [**2**·K^+] and F^- cannot be calculated possibly due to the abstraction of K^+ by F^- leading to the fluctuation of emission spectra and the lower in their intensities. Thus, K^+ bound in 1,3-alternate conformation of **2** cannot facilitate the cooperative effect with F^-. This is due to the topology of the ligand producing a long distance between crown ether and amide group, and reducing electrostatic interactions between K^+ and F^-.

Electrochemical recognition of receptors 1 and 2

Electrochemical studies of receptors **1** and **2** towards anions in the absence and presence of K^+ were examined using cyclic voltammetry. Receptors **1** and **2** show two consecutive one-electron reversible waves in 40% v/v CH_3CN in CH_2Cl_2, corresponding to two single-electron reductions to give mono- and dianion species.[23,24] The chemical reversibility of the voltammetric waves is stable upon varying scan rates which implies that no self-protonation reaction (keto-enol process) intervened their redox reactions. The half-wave potentials for receptors **1** are found at $E_{1/2}$I = −1.21 V and $E_{1/2}$II = −1.66 V while that of **2** are found at $E_{1/2}$I = −1.25 V and $E_{1/2}$II = −1.71 V (Fig. 18 in ESI†). Compared to **2**, the redox waves I and II of receptor **1** shifted towards less negative potentials. This result may stem from the stabilization of the radical anions through the intramolecular hydrogen bonding between the NH amide proton and the crown ether of receptor **1**.[24]

Interestingly, upon addition of 10 equiv. of $H_2PO_4^-$ into the solution of the receptors, waves II of both two receptors shift remarkably toward less negative potentials as shown in Table 3 and Fig. 6. Previous studies showed that dianions (corresponding to wave II) formed were stabilized by the effect of intermolecular hydrogen bonding interactions with the guest, $H_2PO_4^-$.[23,24] Addition of other anions to the solution of receptors results in only insignificant change in reduction potentials of waves I and II.

Addition of K^+ to the solution of the receptors **1** and **2** leads to the positive shift of the reduction potentials in cyclic wave voltammogram as shown in Table 4. The easier reduction of these receptors is due to the stabilization of the reduced quinone species by the presence of metal ions.[45] However, the shift is much larger in receptor **2**. Interestingly, the oxidation peak of the redox wave II in the receptor **2** shows the unique characteristic

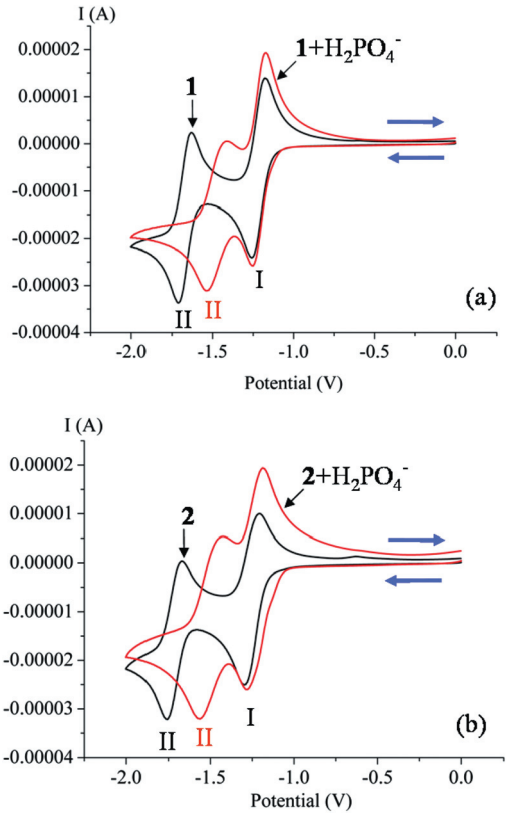

Fig. 6 Cyclic voltammograms of receptor (a) **1** (1 mM) and (b) **2** (1 mM) and $H_2PO_4^-$ (10 equiv.) in 40% v/v CH_3CN in CH_2Cl_2 with 0.1 M $TBAPF_6$ at a scan rate of 50 mV s^{-1}. Blue arrows represent the scan direction.

Table 4 Changes in reduction potentials (mV) of receptors **1** and **2** after addition of 3 equiv. of K^+

	K^+ (3 equiv.)	
Receptors	$\Delta E_{1/2}$ (I)	$\Delta E_{1/2}$ (II)
1	60	95
2	120	305

$\Delta E_{1/2} = E_{1/2\ \text{cation cpx}} - E_{1/2\ \text{free receptor}}$.

peak which is very sharp after adding 3 equiv. of K^+ as shown in Fig. 7. Moreover, after varying the scan rates, the ratio between the intensity of the current of the reduction and the oxidation peak of the redox wave II decreases (close to 1) at higher scan rates. This behavior indicates the kinetic involvement in complexation of **2** with K^+ which could be detected by cyclic voltammetry. This phenomenon is rationalized through the molecular tube characteristic of the 1,3-alternate conformation of calix[4]arene in receptor **2** which can facilitate the K^+ ion to move close to the sensory unit rather than staying only in the crown ether cavity.[46]

To investigate the ion-pair binding ability of these receptors, 3.0 equivalents of K^+ ions were added to the solution of the receptors before adding anions. Upon addition of F^- ion to [**1**·K^+] solution, the wave II of the cation complex [**1**·K^+] shifts

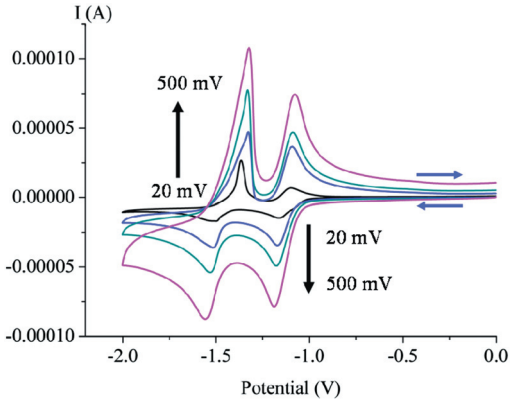

Fig. 7 Cyclic voltammograms of **2** (1 mM) in 40% v/v CH_3CN in CH_2Cl_2 with 0.1 M $TBAPF_6$ at various scan rates (20 mV s^{-1} (black line), 100 mV s^{-1} (blue line), 200 mV s^{-1} (green line) and 500 mV s^{-1} (pink line)). Arrows represent the scan direction.

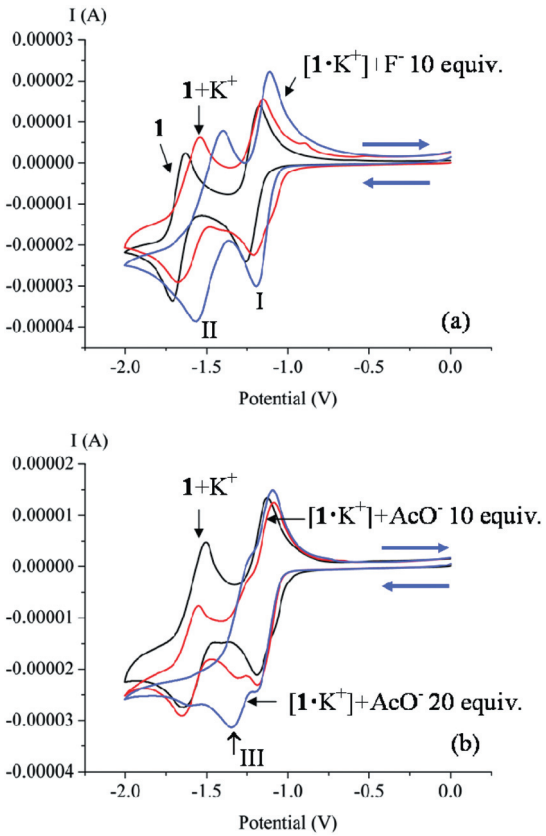

Fig. 8 Cyclic voltammograms of receptor **1** (1 mM) + KPF_6 3.0 equiv. after addition of (a) 10 equiv. F^- and (b) 10 and 20 equiv. AcO^- in 40% v/v CH_3CN in CH_2Cl_2 with 0.1 M $TBAPF_6$ at a scan rate of 50 mV s^{-1}.

to the less negative potentials as shown in Fig. 8. This points to the formation of a stable cobound ion pair in this complex and is pertinent to the results from photophysical studies.

Remarkably, addition of 10 equiv. of AcO^- to [**1**·K^+] solution results in an appearance of a new reversible wave III at −1.35 V which could be ascribed to a cobound ion pair formed during the reduction process. It should be noted that the current intensity of

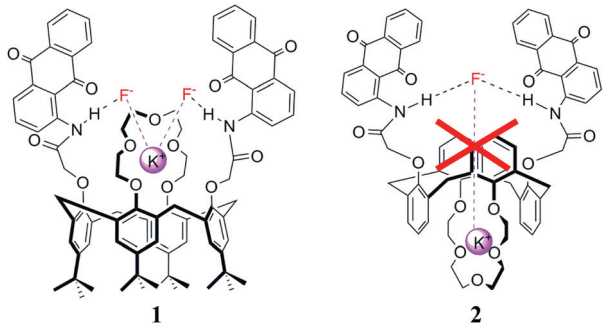

Fig. 9 Proposed structures of co-bound ion pairs. Violet dashed lines represent electrostatic interactions (which are unlikely in the case of receptor **2**).

wave II also decreases. Interestingly, further increasing the amount of AcO^- to 20 equiv. results in the disappearance of wave II and the completion of the redox wave III. Addition of other anions (Cl^-, Br^-, I^- BzO^-) to [**1**·K^+] solution causes only slightly shifts of wave I and wave II. It implies that K^+ and these anions could not form stable enough cobound ion pairs in the CV experiments.

The abstraction of K^+ by anions can even be noticed obviously in [**2**·K^+] system from the reversing of the redox waves of [**2**·K^+] to the original voltammograms of receptor **2** after various anions (F^-, Cl^-, Br^-, AcO^-, $BzO^-$and $H_2PO_4^-$) are added. This result emphasizes that the molecular tube behavior of receptor **2** does not facilitate the cooperative effect of these complexes. In this case, K^+ is removed by negative charges from anions and the reduced anthraquinone probably through the movement in the tube-like 1,3-alternate conformation of calix[4] arene.

As reported previously by Nerngchamnong *et al.*, the topology of the heteroditopic receptors and the presence of metal ions were able to differentiate the anion binding abilities.[31] Similarly, in this study, the results show that the conformation of calix[4]arene plays an important role in anion binding properties of these two heteroditopic receptors. For receptor **1**, the crown ether unit in the cone conformation intersects between the anion binding sites of the receptor. The closer distance between anion and cation binding sites in **1** supports the cooperative binding abilities of **1** towards K^+ and F^- through both electrostatic and hydrogen bonding interactions. However the 1,3-alternate conformation of receptor **2** possessing a longer distance between cation and anion binding sites does not promote the cooperative binding abilities of **2** towards K^+ and various anions, but probably facilitates the abstraction of K^+ as found in ^1H NMR titration, photophysical as well as electrochemical studies. Proposed structures of the two receptors with F^- are, therefore, presented in Fig. 9.

Conclusions

Heteroditopic ion receptors derived from crown ether-based calix[4]arenes containing amido-anthraquinone pendants whereas the conformation of calix[4]arene was in cone and 1,3-alternate conformations, **1** and **2**, respectively were synthesized. In the aspect of dual sensors, both **1** and **2** showed sensing abilities towards

F^- using spectrophotometry. However, both sensors displayed electrochemical sensing abilities towards $H_2PO_4^-$. It was found that the topology of the receptors played a key role in anion binding processes resulting in a closer and a longer distance between a cation and an anion binding sites in **1** and **2**, respectively. Receptor **1** exhibited a dual spectrophotometric and electrochemical sensor for F^- in the presence of K^+ due to the cooperative electrostatic and hydrogen bonding interactions. In addition, cobound **1**·K^+ could detect AcO^- electrochemically (while spectrophotometry could not). On the other hand, receptor **2** did not provide the cooperative binding of K^+ and various anions. This implied that 1,3 alternate conformation of **2** could not deliver electrostatic interactions from its positive charge to anions due to the long distance, but facilitated the abstraction of K^+ by anions.

Experimental

General procedure

All materials and reagents standard analytical grade, and used without further purification. Commercial grade solvents, methanol, dichloromethane, hexane and ethylacetate, were distilled before use. The $CDCl_3$ and CD_3CN were used as internal references for the NMR titration experiment. In anion complexation studies, anions were added as tetrabutylammonium salts.

^1H NMR spectra was recorded with a Varian Mercury 400 NMR spectrometer and a Bruker Avance 400 NMR spectrometer. UV-vis absorption measurements were performed on a Varian Cary 50 Probe UV-Visible Spectrometer. Fluorescence spectra were obtained on a Varian Cary Eclipse fluorescence spectrophotometer. Cyclic voltammetry (CV) was performed using a μ-AUTOLAB TYPE III potentiostat.

Synthesis of heteroditopic receptors 1 and 2

Preparation of compound 1a. The mixture of *p-tert* butylcalix[4]arene (2.00 g, 3.08 mmol) and K_2CO_3 (0.51 g, 3.70 mmol) in 150 mL of dried acetonitrile was refluxed under nitrogen atmosphere for an hour. The solution of tetraethyleneglycol ditosylate, which was prepared from tetraethyleneglycol, (1.86 g, 3.70 mmol) in 50 mL of dried acetonitrile was added dropwise and the mixture was refluxed for 48 hours. Then, K_2CO_3 was removed by filtration. The residue was extracted with CH_2Cl_2 and water. The organic phase was separated and dried over anhydrous $MgSO_4$. The crude product was purified by column chromatography (SiO_2, 20% ethylacetate in hexane). Compound **1a** was precipitated in CH_2Cl_2–MeOH as white solid (1.0 g, 40%). δ_H (400 MHz, $CDCl_3$, ppm) 0.91 (*s*, 18H, *t*Bu), 1.31 (s, 18H, *t*Bu), 3.29 (d, J = 12.8 Hz, 4H, ArCH_2), 3.84 (t, J = 5.2 Hz, 4H, OCH_2), 3.96 (t, J = 5.2 Hz, 4H, OCH_2), 4.08 (s, 8H, OCH_2), 4.37 (d, J = 12.8 Hz, 4H, ArCH_2), 6.75 (s, 4H, Ar*H*), 7.07 (s, 4H, Ar*H*), 7.20 (s, 2H, O*H*); δ_C (100 MHz, $CDCl_3$) 31.0, 31.4, 31.7, 33.8, 33.9, 70.3, 70.9, 71.0, 76.6, 125.0, 125.4, 127.8, 132.5, 141.2, 146.8, 149.8, 150.8; Elemental analysis: calculated for $C_{52}H_{70}O_7$: C, 77.38; H, 8.74, found: C, 77.33; H, 8.73; MALDI-TOF (*m*/*z*) calcd: **1a**: 807.12 found: [**1a**+Na^+]: 829.90.

Preparation of compound 1. The mixture of **1a** (0.50 g, 0.62 mmol) and K_2CO_3 (0.085 g, 0.62 mmol) in 100 mL of dried acetonitrile was heated at reflux under nitrogen atmosphere for 30 min. Bromoacetyl amidoanthraquinone (0.216 g, 0.43 mmol) was added to the mixture and then the mixture was refluxed for 24 hours. Then the reaction was worked up using the same procedure above. The crude product was purified by column chromatography (SiO_2, 20% methanol in dichloromethane). Compound **1** was precipitated in CH_2Cl_2–MeOH as yellow solid (74 mg, 9%). δ_H (400 MHz, $CDCl_3$, ppm) 0.96 (s, 18H, *t*Bu), 1.182 (s, 18H, *t*Bu), 3.27 (d, J = 12.8 Hz, 4H, ArCH_2), 3.30 (s, 4H, OCH_2), 3.53 (s, 4H, OCH_2), 4.21 (t, J = 6.8 Hz, 4H, OCH_2), 4.30 (t, J = 6.8 Hz, 4H, OCH_2), 4.73 (d, J = 12.8 Hz, 4H, ArCH_2), 5.01 (s, 4H, CH_2CO), 6.68 (s, 4H, Ar*H*), 6.96 (s, 4H, Ar*H*), 7.71–7.78 (m, 6H, Ar*H*), 8.05 (d, J = 7.6 Hz, 2H, Ar*H*), 8.28–8.25 (m, 4H, Ar*H*), 9.09 (d, J = 8.4 Hz, 2H, Ar*H*), 12.41 (s_b, 2H); δ_C (100 MHz, $CDCl_3$) 31.2, 31.5, 31.6, 33.7, 33.9, 70.4, 70.7, 71.2, 72.8, 75.1, 118.3, 122.5, 125.1, 125.4, 126.7, 126.9, 127.5, 132.7, 132.9, 134.0, 134.1, 134.2, 134.3, 134.4, 135.3, 141.6, 144.9, 152.0, 154.1, 169.3, 182.7, 186.7; Elemental analysis: calculated for $C_{84}H_{88}N_2O_{13}$: C, 75.65; H, 6.65; N, 2.10 found: C, 75.62; H, 6.60; N, 2.12. MALDI-TOF (*m*/*z*) calcd: **1**: 1333.62, found: [**1**+Na^+]: 1356.48.

Preparation of compound 2a. The mixture of calix[4]arene (0.5 g, 1.18 mmol) and K_2CO_3 (0.48 g, 3.53 mmol) in 150 mL of dried acetonitrile was refluxed under nitrogen atmosphere for half an hour. The solution of bromoacetyl amidoanthraquinone (0.93 g, 2.71 mmol) was added, and the mixture was refluxed for 24 hours. Then the reaction was worked up using the same procedure as above. The crude product was purified by column chromatography (SiO_2, 5% ethylacetate in dichloromethane). Compound **2a** was precipitated in CH_2Cl_2–MeOH as yellow solid (0.35g, 32%). δ_H (400 MHz, $CDCl_3$, ppm) 3.49 (d, J = 14 Hz, 4H, CH_2Ar), 4.44 (s, 4H, CH_2CO), 4.53 (d, J = 14 Hz, 4H, ArCH_2Ar), 5.98 (s, 2H, O*H*), 6.57 (s, 6H, Ar*H*), 6.77 (t, J = 7.2 Hz, 2H, Ar*H*), 7.16 (d, J = 7.2 Hz, 4H, Ar*H*), 7.42 (t, J = 8 Hz, 2H, Ar*H*), 7.48 (t, J = 7.6 Hz, 2H, Ar*H*), 7.55 (t, J = 7.2 Hz, 2H, Ar*H*), 7.73 (t, J = 8 Hz, 4H, Ar*H*), 8.17 (d, J = 7.2 Hz, 2H, Ar*H*), 8.48 (d, J = 8 Hz, 2H, Ar*H*), 13.172 (s_b, 2H, N*H*); δ_C (100 MHz, $CDCl_3$) 30.6, 74.4, 117.7, 119.2, 123.0, 124.7, 125.7, 126.5, 127.6, 128.7, 129.0, 129.7, 131.9, 132.3, 133.1, 133.2, 133.7, 134.2, 135.5, 140.0, 152.7, 153.2, 167.7, 181.3, 186.2; Elemental analysis: calculated for $C_{60}H_{42}O_{10}N_2$: C, 75.78; H, 4.45; N, 2.95, found: C, 75.50; H, 4.47; N, 2.94; MALDI-TOF (*m*/*z*) calcd: **2a**: 950.98, found: [**2a**+K^+]: 990.22.

Preparation of compound 2. The mixture of **2a** (0.2 g, 0.2 mmol) and Cs_2CO_3 (0.64 g, 1.96 mmol) in 100 mL of dried acetonitrile was refluxed under nitrogen atmosphere for half an hour. The solution of tetraethyleneglycol ditosylate (1.0 g, 1.98 mmol) in 20 mL of dried acetonitrile was added dropwise, and the mixture was refluxed for 24 hours. Then, Cs_2CO_3 was removed by filtration. Then the reaction was worked up using the same procedure above. The crude product was purified by column chromatography (SiO_2, 5% methanol in dichloromethane). Compound **2** was precipitated in CH_2Cl_2–MeOH as yellow solid (15 mg, 7%). δ_H (400 MHz, $CDCl_3$,) 3.20 (t, J = 6.8 Hz, 4H, CH_2O), 3.38 (s, 4H, CH_2O), 3.66–4.37 (m, 12H,

CH_2O), 3.90 (d, J = 16.4 Hz, 4H, ArCH_2Ar), 4.20 (d, J = 16.4 Hz, 4H, ArCH_2Ar), 6.71 (t, J = 7.2 Hz, 2H, Ar*H*), 6.94 (t, J = 7.6 Hz, 2H, Ar*H*), 7.03 (d, J = 7.6 Hz, 4H, Ar*H*), 7.19 (d, J = 7.6 Hz, 4H, Ar*H*), 7.61 (t, J = 8 Hz, 2H, Ar*H*), 7.76–7.74 (m, 4H, Ar*H*), 8.04 (d, J = 7.6 Hz, 2H, Ar*H*), 8.29–8.23 (m, 4H, Ar*H*), 8.95 (d, J = 8.4 Hz, 2H, Ar*H*), 12.23 (s_b, 2H, N*H*); δ_C (100 MHz, $CDCl_3$) 38.2, 68.6, 69.5, 71.0, 71.3, 73.0, 118.7, 122.6, 123.2, 123.8, 126.8, 126.9, 127.4, 130.2, 130.3, 132.7, 134.1, 134.13, 134.2, 134.26, 134.3, 135.0, 135.2, 141.3, 154.9, 156.7, 169.5, 182.9, 186.2; Elemental analysis: calculated for $C_{68}H_{56}N_2O_{13}$: C, 73.61; H, 5.08; N, 2.52; found: C, 73.48; H, 5.12; N, 2.61; MALDI-TOF (*m*/*z*) calcd: **2**: 1109.20 Found [**2**+K^+] = 1148.81.

NMR titrations

Solutions of **1** and **2** (0.005 M) in 5% v/v CD_3CN in $CDCl_3$ (0.5 mL) were prepared in NMR tubes. A 0.05 M stock solution of any anionic guest molecules in 5% v/v CD_3CN in $CDCl_3$ was prepared in a small vial. The solution of guest molecules was gradually added into the NMR samples *via* a micro syringe.

Photophysical studies

Solutions of **1** and **2** (5.0×10^{-5} M) were prepared and pipetted into a 1 cm pathlength quartz cuvette. The absorption spectra were recorded in the range of 200–800 nm. Fluorescence spectra were recorded with the width of the excitation slit and the emission slit at 10 nm and excited at 450 nm. Anions or a cation were gradually added to quartz cuvette and stirred for a few minutes before each run. The binding constants between the ligand and various ions were determined by SPECFIT32 software.

Electrochemical studies

Solutions of **1** and **2** (1.0×10^{-3} M) were prepared and poured into a cell. Cyclic voltammetry experiments were carried out with three electrode cells. A glassy carbon electrode was used as a working electrode. The surface of the working electrode was polished with slurries of 1.0 μm followed with 0.3 μm alumina powder, and then rinsed with water. Residual alumina particles were thoroughly removed by sonicating the working electrode for 5 min in 0.05 M H_2SO_4. The electrode was then rinsed successively with water and acetone, and dried. A Pt wire was used as a counter electrode. The Ag–$AgNO_3$ electrode, constructed by immersing a silver wire into a solution of 0.01 M $AgNO_3$ in 0.1 M $TBAPF_6$, was used as a reference electrode. The supporting electrolyte is 0.1 M tetrabutylammonium hexafluorophosphate ($TBAPF_6$) in 40% v/v CH_3CN in CH_2Cl_2. The solution of tested compounds were flushed with N_2 gas for 5 min before performing the experiment. Experiments were performed at room temperature at a scan rate of 50 mV s^{-1}.

Acknowledgements

We would like to thank Development and Promotion of Science and Technology talents project (DPST) and the Thailand Research Fund (RTA5380003) for financial support. We gratefully acknowledged Dr Chomchai Suksai for helpful discussion in analysis of titration data using SPECFIT32.

Notes and references

1 A. K. Mishra, J. Jacob and K. Müllen, *Dyes Pigm.*, 2007, **75**, 1.
2 N. Kaur and S. Kumar, *Tetrahedron Lett.*, 2006, **47**, 4109.
3 N. Kaur and S. Kumar, *Dalton Trans.*, 2006, 3766.
4 H. J. Kim, S. J. Lee, S. Y. Park, J. H. Jung and J. S. Kim, *Adv. Mater.*, 2008, **20**, 3229.
5 S.-P. Wu, K.-J. Du and Y.-M. Sung, *Dalton Trans.*, 2010, **39**, 4363.
6 E. Ranyuk, C. M. Douaihy, A. Bessmertnykh, F. Denat, A. Averin, I. Beletskaya and R. Guilard, *Org. Lett.*, 2009, **11**, 987.
7 Y.-J. Zhang, X.-P. He, M. Hu, Z. Li, X.-X. Shi and G.-R. Chen, *Dyes Pigm.*, 2011, **88**, 391.
8 N. Kaur and S. Kumar, *Tetrahedron*, 2008, **64**, 3168.
9 N. Kaur and S. Kumar, *Chem. Commun.*, 2007, 3069.
10 H. J. Kim, H. S. Kim, J. H. Kim, L. N. Anh, J. H. Lee, C.-H. Lee and J. S. Kim, *Tetrahedron Lett.*, 2009, **50**, 2782.
11 S. H. Kim, H. S. Choi, J. Kim, S. J. Lee, D. T. Quang and J. S. Kim, *Org. Lett.*, 2010, **12**, 560.
12 D. Y. Han, J. M. Kim, J. Kim, H. S. Jung, Y. H. Lee, J. F. Zhang and J. S. Kim, *Tetrahedron Lett.*, 2010, **51**, 1947.
13 H. Yang, Z.-G. Zhou, J. Xu, F.-Y. Li, T. Yi and C.-H. Huang, *Tetrahedron*, 2007, **63**, 6732.
14 X. Peng, Y. Wu, J. Fan, M. Tian and K. Han, *J. Org. Chem.*, 2005, **70**, 10524.
15 S. Kumar, V. Luxami and A. Kumar, *Org. Lett.*, 2008, **10**, 5549.
16 R. M. F. Batista, E. Olivira, S. P. G. Costa, C. Lodeiro and M. M. M. Raposo, *Org. Lett.*, 2007, **9**, 3201.
17 D. Jiménez, R. Martinez-Máñez, F. Sancenón and J. Soto, *Tetrahedron Lett.*, 2002, **43**, 2823.
18 D. A. Jose, D. K. Kumar, B. Ganguly and A. Das, *Org. Lett.*, 2004, **6**, 3445.
19 F.-Y. Wu, M.-H. Hu, Y.-M. Wu, X.-F. Tan, Y.-Q. Zhao and Z.-J. Ji, *Spectrochim. Acta, Part A*, 2006, **65**, 633.
20 H. S. Jung, H. J. Kim, J. Vicens and J. S. Kim, *Tetrahedron Lett.*, 2009, **50**, 983.
21 F. J. Gonzàlez, *Electroanalysis*, 1998, **10**, 638.
22 T. Ossowski, P. Pipka, A. Liwo and D. Jeziorek, *Electrochim. Acta*, 2000, **45**, 3581.
23 N. Gupta and H. Linschitz, *J. Am. Chem. Soc.*, 1997, **119**, 6384.
24 M. Gomóz, F. J. González and I. González, *J. Electroanal. Chem.*, 2005, **578**, 193.
25 S. J. Brooks, P. R. Birkin and P. A. Gale, *Electrochem. Commun.*, 2005, **7**, 1351.
26 M. Alfonso, A. Tárraga and P. Molina, *J. Org. Chem.*, 2011, **76**, 939.
27 M. Alfonso, A. Espinosa, A. Tárraga and P. Molina, *Org. Lett.*, 2011, **13**, 2078.
28 F. Zapata, A. Caballero, A. Tárraga and P. Molina, *J. Org. Chem.*, 2010, **75**, 162.
29 F. Otón, A. Tárraga and P. Molina, *Org. Lett.*, 2006, **8**, 2107.
30 M. Hardouin-Lerouge, B. Chesneau, M. Allain and P. Hudhomme, *J. Org. Chem.*, 2012, **77**, 2441.
31 N. Nerngchamnong, B. Chailap, P. Leeladee, O. Chailapakul, C. Suksai and T. Tuntulani, *Tetrahedron Lett.*, 2011, **52**, 2914.
32 S. Suksai, P. Leeladee, D. Jainuknan, T. Tuntulani, N. Muangsin, O. Chailapakul, P. Kongsaeree and C. Pakavatchai, *Tetrahedron Lett.*, 2005, **46**, 2765.
33 J. L. Sessler and S. K. Kim, *Chem. Soc. Rev.*, 2010, **39**, 3784.
34 S. K. Kim, J. L. Sessler, D. E. Gross, C.-H. Lee, J. S. Kim, V. M. Lynch, L. H. Delmau and B. P. Hay, *J. Am. Chem. Soc.*, 2010, **132**, 5827.
35 P. D. Beer and P. A. Gale, *Angew. Chem., Int. Ed.*, 2001, **40**, 486.
36 P. A. Gale, *Coord. Chem. Rev.*, 2003, **240**, 191.
37 P. D. Beer and E. J. Hayes, *Coord. Chem. Rev.*, 2003, **240**, 167.
38 J. M. Mahoney, G. U. Nawaratna, A. M. Beatty, P. J. Duggan and B. D. Smith, *Inorg. Chem.*, 2004, **43**, 5902.
39 P. A. Gale, S. E. García-Garrido and J. Garric, *Chem. Soc. Rev.*, 2008, **37**, 151.
40 M. D. Lankshear, I. M. Dudley, K. M. Chan, A. R. Cowley, S. M. Santos, V. Fejix and P. D. Beer, *Chem.–Eur. J.*, 2008, **14**, 2248.
41 A. Senthilvelan, I.-T. Ho, K.-C. Chang, G.-H. Lee, Y.-H. Liu and W.-S. Chung, *Chem.–Eur. J.*, 2009, **15**, 6152.

42 C. Jaime, J. Mendoza, P. Prados, P. M. Nieto and C. Sanchez, *J. Org. Chem.*, 1991, **56**, 3372.
43 R. S. Macomber, *J. Chem. Educ.*, 1992, **69**, 375.
44 J. K. Choi, S. H. Kim, J. Yoon, K.-H. Lee, R. A. Bartsch and J. S. Kim, *J. Org. Chem.*, 2006, **71**, 8011.
45 N. Kerdpaiboon, B. Tomapatanaget, O. Chailapakul and T. Tuntulani, *J. Org. Chem.*, 2005, **70**, 4797.
46 B. Pulpoka, L. Baklouti, J. S. Kim and J. Vicens, in *Calixarenes in the Nanoworld*, ed. J. Vicens and J. Harrowfield, Springer, 2007, pp. 135–149 and references therein.